



Thermal characteristics and combustion reactivity of coronavirus face masks using TG-DTG-MS analysis

Nebojša Manić¹ · Bojan Janković² · Dragoslava Stojiljković¹ · Panagiotis Angelopoulos³ · Miloš Radojević¹

Received: 16 November 2021 / Accepted: 1 April 2022 / Published online: 3 May 2022
© Akadémiai Kiadó, Budapest, Hungary 2022

Abstract

The presented paper deals with the influence of the heating rate on combustion characteristics (reactivity and reactivity evaluation, ignition index (D_i), burnout index (D_p), the combustion performance index (S), and the combustion stability index (R_w)) of the protective coronavirus face masks. Two types of commonly used face masks in different state (new and exploited) were investigated by TG-DTG analysis in an air atmosphere, directly coupled with mass spectrometry (MS). Based on the experimental results, the impact of ultimate and proximate analysis data on the evolved gas analysis (EGA) was discussed. Also, the derived values from thermo-analytical (TA) data were compared with the literature reports, related to individual constitutive face mask materials. According to the performed research, it was established that different maximal reaction rate values at various heating rates indicate the complex nature of coronavirus face mask thermo-oxidative degradation, which is stimulated with carbon oxidation reactions and volatile matter (VM) release. By detailed analysis of obtained TG-DTG profiles, it was established that process takes place through the multiple-step reaction pathways, due to many vigorous radical reactions, causes by polymers degradation. The performed research was done to evaluate the possible utilization of coronavirus waste to energy production and sustainable pandemic environmental risk reduction.

Keywords Coronavirus face mask · TG-DTG-MS · Combustion · Thermal analysis properties · Heating rate

Introduction

Disposable surgical face masks have been highly sought-after commodity in recent months, so millions of them are sold, used, and then inevitably end up in the garbage. We have also seen cases where they used to clog sewage systems in cities, and thrown in the garbage will very often end up in nature, oceans or in the country, where they will not decompose for many years to come. The latest study by Jain et al. [1] shows that that disposable masks made of polypropylene, could be doubly useful. Once they fulfill their primary purpose of protecting people from viruses

penetrating their respiratory organs (current situation with COVID-19 disease caused by coronavirus), they could be collected and recycled, instead of becoming environmental pollutants. If they are decomposed by pyrolysis, biodiesel could be obtained from them, a synthetic biofuel that can be a very good source of energy. The cited study suggests efficient and economical recycling of these protective masks by pyrolysis process, where through breaking of long-chain polymer molecules into the simple, smaller molecules, can be obtained biofuel, after a process of 60 min, at the temperatures of 300–400 °C. This process does not require that the protective equipment is separated according to the types of materials, because it is able to convert a mixture of different plastics into biofuel. If we know that disposable protective masks are being produced more and more, and it is likely that this trend will continue, and we add to this the constantly growing global need for new sources of clean energy, recycling plastic masks into biofuel seems like a very interesting solution. Research has shown [1] that obtained liquid fuel via pyrolytic conversion has very similar properties to fossil fuels, so the recommendation was to start pyrolysis of waste protective equipment as soon as possible, in order to

✉ Nebojša Manić
nmanic@mas.bg.ac.rs

¹ Faculty of Mechanical Engineering, Fuel and Combustion Laboratory, University of Belgrade, Belgrade, Serbia

² Department of Physical Chemistry, Vinča Institute of Nuclear Sciences - National Institute of The Republic of Serbia, University of Belgrade, Belgrade, Serbia

³ School of Mining and Metallurgical Engineering, National Technical University of Athens, Athens, Greece

solve both problems at the same time—the accumulation of plastic waste and the lack of “green” fuel. In this paper, a conversion study of the personal protection equipment (PPE) such as face masks (coronavirus protective face masks) via combustion process (in the presence of oxygen supply) was performed, using thermo-analytical (TA) techniques, coupled mass spectrometry (MS) for the analysis of gaseous products.

This study aims to investigate the thermo-oxidative degradation of two kinds of unused and used coronavirus protective face masks to estimate their possible energy potential, using the lab-scale experiments by the thermal analysis techniques such as thermogravimetry (TG)—derivative thermogravimetry (DTG) coupled with mass spectrometry (MS) analysis. In addition, the combustion characteristics parameters evaluated in the current work can help in assessing the improvement or deterioration of the process in question of environmental pollution issues, when this type of waste is considered for use in the possible energy purposes.

The face mask samples used in this study were chosen not only to assess the energy potential of various types of face masks but also to determine the impact of the face mask's application as a piece of protective equipment on its potential for utilization for production energy. In this regard, two types of face masks were tested: the traditional (surgical) face mask, which is most often used for pandemic protection around the world, and as declared extra protective face mask (against covid-19) with a zeolite layer and silver ions. For both types, the “new” and “used” samples were examined. The “new” sample was made from face masks purchased in a local drug shop and opened directly from the product package, while the “used” sample was collected from a container intended for this type of medical waste, following all safety and health procedures and standards. The face masks that were disposed of and used for the processing of the “used”

sample, was assumed to have been applied according to the instructions for use on the product packaging, which specifies a total length of 3 h of wearing masks before disposal in a medical waste container. Table 1 shows the appearance of the two types of face masks used in this study.

The first sample represents new manufactured commercial surgical face mask marked as M1 (treated as medical waste after use) and its corresponded replicate sample M1-USED, which represents a used mask after 3 h of respiration. Based on manufacturers product declarations surgical face mask (M1) by its composition contains about 55% of fibrous material (cotton fibers) and 45% of polymeric material-polypropylene (PP). The second sample represents new manufactured commercial coronavirus protective face mask (M2, Table 1) which represents the non-disposable face mask, which can be washed several times, and based on product declaration has a different composition than the M1 face mask. This mask contains about 35% of fibrous material (cotton fibers), 40% of polypropylene (PP), and 25% of natural zeolite-clinoptilolite ($(K_2, Na_2, Ca)_3[Al_6Si_3O_{72}]$) a member of the heulandite group (HEU) of zeolites, and silver (Ag) ions impregnated by the surface coating. Its replicate sample represents M2-USED, which is the used mask after 3 h of respiration (Table 1).

Based on the literature overview, the detailed chemical composition for 3- and 4-layered face masks commonly used as a protective equipment against COVID-19, is presented in Table 2.

As can be seen from Table 2 the chemical composition of protective face masks varies in dependence of type, the part of the face mask as well as of the manufacturer layer arrangements. Those composition variations are highly related to the combinations of raw materials selection within the face mask production process, but also could significantly influence the possible pathway for its utilization [4].

Table 1 Tested face mask samples



Sample	Description	Image
M1	The commercial surgical face mask—new	
M1-USED	The commercial surgical face mask—used	
M2	The extra protective face mask with zeolite and silver ions—new	
M2-USED	The extra protective face mask with zeolite and silver ions—used The maximum value of the DTG curve increased with an increasing of heating rates, which caused a higher value of the peak temperature	

Table 2 Overview of chemical composition of protective COVID-19 face masks

	Cellulose/ mass%	Cellu- lose + poly- olefin/mass%	Felt/ mass%	Polyolefin/ mass%	PP ^a / mass%	PP/PE ^b / mass%	Nylon/ mass%	Metals/ mass%	Ref.
Surgical face masks									
Inner layer	9.09	3.03	3.03	–	69.70	15.15	–	–	[2]
Middle layer	–	3.03	3.03	–	81.82	12.12	–	–	[2]
Outer layer	–	3.03	3.03	6.06	78.79	9.09	–	–	[2]
Disposable face mask(KF94 grade)									
Filter layers 1, 3, 4	–	–	–	–	73.33	–	–	–	[3]
Filter layer 2	–	–	–	–	–	13.77	–	–	[3]
Ear strap	–	–	–	–	–	–	8.27	–	[3]
Nose frame	–	–	–	–	–	–	–	4.63 ^c	[3]

^aPolypropylene (PP)^bPolyethylene (PE)^c(Fe: 4.58, Zn: 0.02, Ti: 0.01, Ca: 0.01 and Mn: 0.01)

It could be clearly observed that aside from the direct health concerns, the treatment and prevention of COVID-19 resulted in a significant amount of medical waste. This could cause environmental issues, particularly in terms of waste management and landfill disposal. In this regard, the authors of this study attempted to identify a feasible strategy for utilizing the high amount of medical waste generated, as well as its potential for energy production. Besides, the identification of thermal degradation of considered material that could be possibly used in the combustion/incineration process is essential for planning and developing the possible material/fuel utilization pathway. The TG-DTG analysis directly coupled with the MS analysis presented in this manuscript together with the determination of thermal characteristics and combustion parameters could provide more information for possible utilization of the considered materials. Also, the specific material characteristics on which are point in within this research should be identified and could provide new insights for the performing of the utilization process. The analysis of evolved gasses from the coupled MS experiments could lead to better planning and analyzing the energy and the environmental issues during the process of thermal degradation. In accordance with all the above-mentioned Authors within this manuscript performed the analysis for the waste material which amount is in the time of global pandemic could not be neglected and provided the information of the thermal degradation characteristics and special combustion parameters which are useful for possible utilization and solving the raised environmental problem.

Materials and methods

After collecting, the all face mask samples are prepared for the experimental research according to the detailed procedure given by standard guidelines and procedures which were applied for this type of waste material for possible energy production [5]. These procedures enable the forming of a homogenous and representative sample for further characterization and it is based on standard analytical techniques for the sample preparation with the statistical approach. By following those guidelines, the examined sample represents the material from the bulk which is considered. Furthermore, the considered face mask samples were shredded and sieved according to the standard procedures [6] for the waste material potential to be used for energy production. Also, based on a set of standard analytical procedures defined in the ref. [6], the data of proximate and ultimate analysis for all samples were collected. The simultaneous thermal analyzer NETZSCH STA449F5 Jupiter directly coupled with mass spectrometer NETZSCH QMS403D Aëolos were used for thermal analysis of considered face mask samples. The sample masses of $\Delta m = 10 \pm 0.5$ mg were placed in alumina crucibles, and heated from the room temperature (RT) to 600 °C, using the heating rates of $\beta = 5, 10, 20, \text{ and } 30 \text{ K min}^{-1}$. In order to avoid the effects of heat and mass transfer limitations, the particle size was under

250 μm , which was achieved using the appropriate sieve size of 60 Mesh. The oxidizing atmosphere was used, in measurements, where the air (21 vol.% oxygen and 78 vol.% nitrogen) represents the purge gas with a flow rate of $\varphi = 70 \text{ mL min}^{-1}$. The mass spectrometry analysis was performed on the quadrupole mass sensor directly coupled with a simultaneous thermal analyzer to determine the following amu's 2, 12, 15, 17, 18, 26, 27, 29, 30, 39, 41, 42, 43, 44, 45, and 58 by bar graph cycles. The selection and further analysis of monitoring amu's were done according to the previous work of authors [7] and data from NIST database in order to identify the evolved gasses of interests for the energy utilization of tested face mask samples (H_2 , H_2O , CO_2 , and light hydrocarbons). The calculation of all considered combustion parameters for tested samples was done according to the mathematical expressions given by Aich et al. [8].

Results and discussion

Results of proximate and ultimate analysis

Table 3 shows proximate and ultimate analysis results of the face masks used in this study. The results include unused (M1 and M2), and used (M1-USED and M2-USED) protective face mask samples.

Both samples (in pairs M1–M1-USED and M2–M2-USED) have low moisture content (below 1%), except for M2-USED sample after respiration (moisture equal to 1.17%), indicating that this face mask after respiration retains slightly more moisture due to the presence of zeolite material which is a porous material capable of absorbing a larger amount of water. M1/M1-USED samples are characterized by a high volatile matter (VM) contents (Table 3), while M2/M2-USED samples have a slightly lower content of VM, which is strongly conditioned by their chemical composition, since they contain a larger amount of inorganic ingredients, which are not volatile and remaining as a solid residue (much higher ash content, Table 3). This is also reflected in the larger content of fixed carbon (FC) for M2/M2-USED samples in the comparison with values of FC related to M1/M1-USED samples. As shown in Table 3, carbon (C) and hydrogen (H) represent the major elements in the tested samples with average concentrations of 85.15 mass% and 12.28 mass% (M1/M1-USED) and 60.62 mass% and 11.10 mass% (M2/M2-USED), respectively. The fibrous-rich face mask such as M1 was characterized with much higher C content than zeolite-rich face mask (M2), which is also reflected on the hydrogen (H) contents, but this difference is not significantly large, if the carbon content is taken under consideration. Compared M1 and M2 face masks, it seems that M1 face masks should

Table 3 Proximate and ultimate analysis of tested samples

Proximate analysis/mass%		Ultimate analysis ^a /mass%	
Sample: M1			
Moisture	0.51	C	85.53
Volatile matter	98.39	H	12.19
Ash	0.45	O ^b	1.65
Fixed carbon	0.65	N	0.18
		S	0.00
HHV, MJ kg ⁻¹	45.42	H/C	1.71
LHV, MJ kg ⁻¹	42.74	O/C	0.01
Sample: M1-USED			
Moisture	0.96	C	84.76
Volatile matter	96.30	H	12.36
Ash	0.40	O ^b	2.35
Fixed carbon	0.84	N	0.12
		S	0.00
HHV, MJ kg ⁻¹	44.98	H/C	1.75
LHV, MJ kg ⁻¹	42.27	O/C	0.02
Sample: M2			
Moisture	0.71	C	60.67
Volatile matter	79.45	H	10.92
Ash	18.59	O ^b	9.38
Fixed carbon	1.25	N	0.31
		S	0.00
HHV, MJ kg ⁻¹	35.75	H/C	2.16
LHV, MJ kg ⁻¹	33.35	O/C	0.12
Sample: M2-USED			
Moisture	1.17	C	60.57
Volatile matter	79.32	H	11.28
Ash	17.96	O ^b	9.72
Fixed carbon	1.55	N	0.25
		S	0.00
HHV, MJ kg ⁻¹	34.89	H/C	2.24
LHV, MJ kg ⁻¹	32.43	O/C	0.12

^aOn a dry basis

^bBy the difference

be a much better source of carbon precursor than M2 ones. For both type of face masks, the sulfur (S) is completely absent, while the nitrogen (N) content in the case of M2/M2-USED samples is slightly higher than N content related to M1/M1-USED samples. However, the N content for M1/M1-USED samples is almost twice as low as N content for M2/M2-USED samples. This ensures that no toxic emissions (e.g., SO_2 and NO_x) can be produced during thermochemical treatment at large-scale of M1 type face masks, which could not be argued for M2 type face masks (see Table 3). The differences between these two types of samples can also be seen in the oxygen (O) content, since that M2/M2-USED samples possess much higher oxygen (O) content which is

clearly reflected in O/C atomic ratio values listed in Table 3. This can make a significant difference in the classification of these masks as future synthetic fuels (their position on the Van Krevelen diagram for fuel classifications). Unlike zeolite/Ag riches PPE, the fibrous-riches PPE (M1/M1-USED samples (Table 3)) contains a huge amount of volatile matter up to ~98.39 mass%, with little ash content with average value of 0.43 mass%. This very high VM content contributes to conversion process and increase in the heating value of synthesized fuel (Table 3). The HHV and LHV values for M1/M1-USED samples are extremely high, which fits calorific values for petrol (benzine) fuel (45–47 MJ kg⁻¹), but with far greater values of HHV than HHVs related to other waste materials, such as medical waste (19–24 MJ kg⁻¹), the industrial and hazardous waste (22–40 MJ kg⁻¹), domestic waste (without the recycling) (7–16 MJ kg⁻¹), domestic waste (after the recycling) (10–14 MJ kg⁻¹), dry wood (14.4 MJ kg⁻¹), paper (13.5 MJ kg⁻¹), and brawn carbon (7–12 MJ kg⁻¹) [9]. Resulted HHV value for M1 sample

approaches to calorific value of diesel (~46 MJ kg⁻¹). In addition, various types of coal fuels are limited in the range of $0 \leq H/C \leq 0.10$ and $0 \leq O/C \leq 0.30$, whereas biomass fuels having a higher proportion of O/C are categorized in the limits of $0.70 \leq O/C \leq 1.30$ and $0.075 \leq H/C \leq 0.25$. It can be seen from presented results in Table 3 that H/C ratios for all investigated samples exceed ranges of H/C limits for coal and biomass fuels, while O/C ratios belong approximately within limits of O/C values related to coal fuels. On the other hand, the higher ash (A) contents related to M2/M2-USED samples may act as catalyst leading to changed reactivity of substances to be activated, so, investigated samples should show different thermo-oxidative reactivity during combustion processes and their combustion properties. Based on significant compositional diversity among samples, it can be preliminary concluded that during thermochemical conversion, different amounts of formulated gaseous and liquid products may be obtained, affecting different energy yields (M1 sample is richer with lignocellulose components such

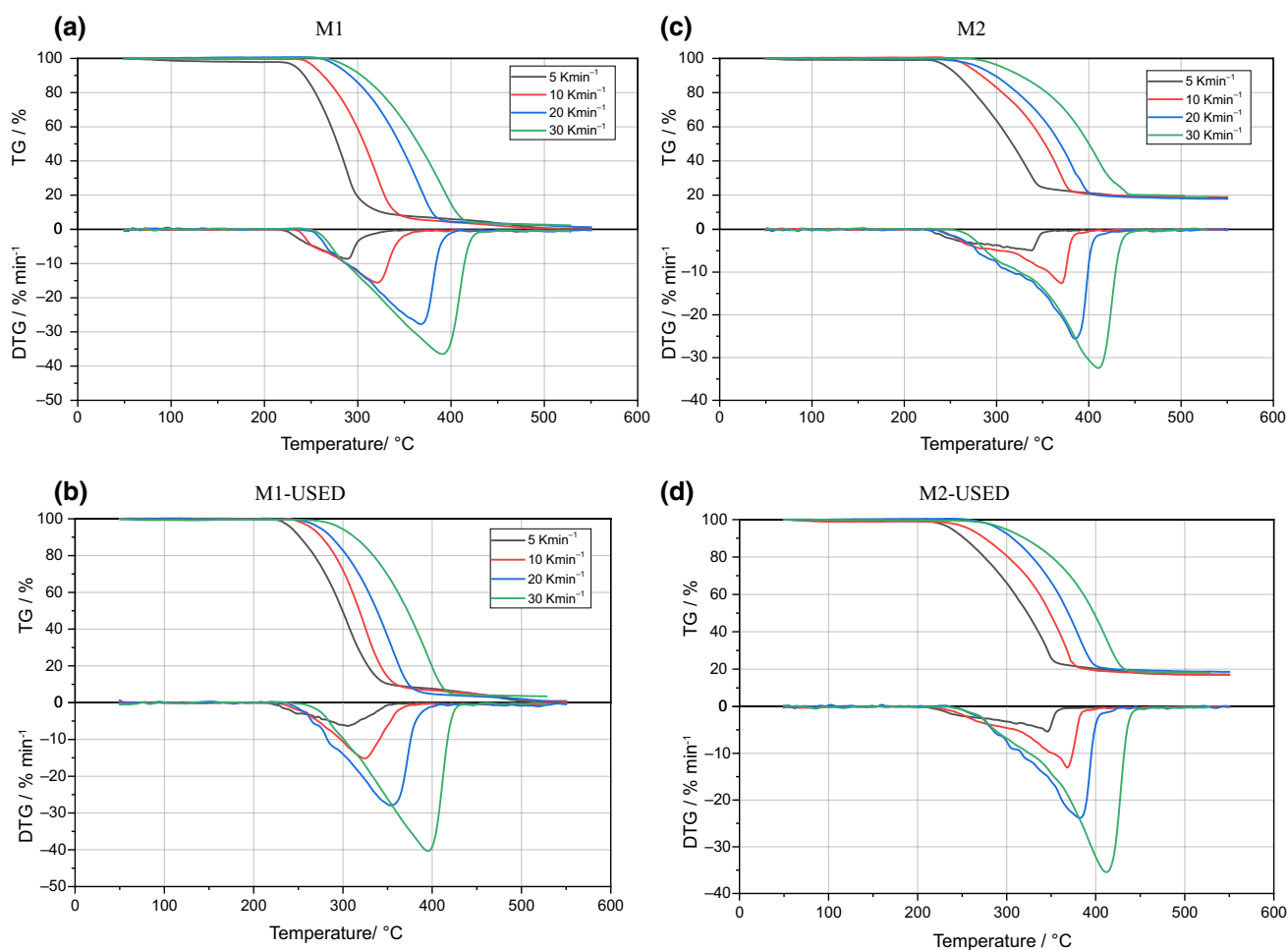


Fig. 1 TG-DTG profiles for **a** M1, **b** M1-USED, **c** M2 and **d** M2-USED milled face masks during the combustion process, in an air atmosphere at $\beta = 5, 10, 20$ and 30 K min^{-1}

as cellulose and hemicelluloses, unlike M2 sample, which is richer with metallic compounds).

TG-DTG reaction profiles and combustion characteristics of tested samples

Figure 1a–d shows TG-DTG profiles of M1, M1-USED, M2 and M2-USED milled face masks in the temperature ranges from 50 to 560 °C, and different heating rates in the scope of $\beta=5, 10, 20$ and 30 K min^{-1} , in an air atmosphere.

Considering obtained thermo-analytical (TA) profiles, because the negligible thermal degradation (mass change) was shown below 200 °C and above 550 °C, the mass loss and DTG curves were selectively described from 200 to 550 °C. Since that both type of masks contains one major polymeric constituent (i.e., the polypropylene (PP)), the phase transition flow value of PP is around 160 °C [10]. Since that the PP is incorporated in two outside and one inside filter layers of M1 disposable surgical face mask, this polymeric component enters in the largest mass loss (Fig. 1). DTG curves for all samples and at all heating rates show the pronounced single maximum-rate peak, whose position depends on the applied heating rate. Considering all tested samples, the position of TG curves and maximum rate temperatures are shift to a higher temperature zones as the heating rate increases, indicating that the effect of heating rate on the value of reaction rate is smaller than that of temperature. The increase in β causes an increase in the thermo-oxidative rate for all considered samples, where combustion intensifies increasing the heating rate magnitudes. However, DTG curves of combustion process for all samples shows appearance of “shoulder” feature which spreads in the temperature range of 250–350 °C (for M1/M1-USED) and 225–375 °C (for M2/M2-USED) (Fig. 1). However, for M2/M2-USED samples, this “shoulder” is much more pronounced. The appearance of this “shoulder” in the DTG curves of these samples is similar to the appearance of the thermo-analytical “shoulder” during the thermochemical conversion of the cellulosic (fibrous) material, as in the case of thermal decomposition of biomass feedstock. Therefore, based on the reactivity shape of TG-DTG features, the main combustion stage belongs to the PP degradation with imposed degradation reactions of fibrous material dispersed in the PP matrix. This can be validated since that combustion process proceeds via overlapping reaction pathway, where the main reaction can be attributed to the PP combustion process, situated about 400 °C where this value depends on the heating rate (Fig. 1) [11]. This agrees with thermal stability studies for microplastic determinations of different polymers [10].

Considering DTG profiles of both types of face masks used in this study (M1/M1-USED and M2/M2-USED), the DTG curves for M2/M2-USED samples are sharper, while DTG curves for M1/M1-USED samples show a more

“diffusion-extended” character (Fig. 1). The influence of heating rate on the distribution of temperature values in different combustion process zones, influencing the shape of thermo-analytical curves is reflected through characteristic temperatures such as *ignition temperature* (T_{ig}) (T_{ig} presented the temperature at which the sample begins to burn), *burnout temperature* (T_b) (T_b presented the point at which fuel oxidation was finished, and it was defined as the temperature where the sample mass loss corresponded to 98 mass% of the initial mass of the sample) and *maximum peak temperature* (T_p) (the maximum peak temperature, T_p , can be identified by using a DTG curve, and it presented the maximum rate of the mass loss of the sample). Unlike DTG curves related to M1/M1-USED samples, the M2/M2-USED samples exhibit DTG curves which were characterized by a shorter DTG_{max} peak compared to previously ones, which was induced by the devolatilization process, which proceeded the more slowly (Fig. 1). The appropriate values of characteristic combustion temperatures are listed in Table 4.

The T_p values for both M2 and M2-USED samples are higher than T_p values of M1 and M1-USED samples, as well as this behavior stays for burnout temperature (T_b) values. On the other hand, the T_{ig} value is somewhat moderated. Namely, T_{ig} (M2 sample) $>$ T_{ig} (M1 sample), while for used face masks, the following situation is valid: T_{ig} (M1-USED) $>$ T_{ig} (M2-USED). The increasing of the heating rate strongly influenced the reactivity of all samples under the monitored atmosphere. This caused the process to move toward higher temperature, and maximal mass rates were increased. This means that creation of a volatile cloud does not take place and does not exist any prevention of the oxygen absorption toward the investigated material. Considering the established T_p and T_b values, which were higher for unused and used M2 type of face mask than T_p and T_b values for M1 and M1-USED samples, it can be concluded that both M2 face mask samples exhibit the lower reactivity compared to M1 face masks. This may have been caused by a higher content of inorganic matter presented in the M2 type of face mask, which possibly had an influence on the heat transfer in the testing thermo-balance chamber. The influence of ash (A) content (Table 3) on the T_{ig} could be observed from the difference in ΔT_{ig} change. Namely, the ignition temperature increased (by 16–57 °C), while the ash content increased (by 18.14 mass%) comparing the samples M2 and M1 (Table 4), with addition of zeolite-metallic ions in a polymer basic matrix of face mask. On the other hand, very small change in the ash content in a decreased direction from 0.45 to 0.40 mass% (M1 \rightarrow M1-USED) and from 18.59 to 17.96 mass% (M2 \rightarrow M2-USED) caused inverse transformation of T_{ig} (M1-USED) $>$ T_{ig} (M2-USED), which may indicates changes in the volatiles content in used face masks in respect to unused masks during combustion process, taking into consideration the trend in T_b values. Furthermore,

Table 4 Characteristic combustion temperatures of tested samples (M1/M1-USED and M2/M2-USED face masks)

		M1	5	10	20	30	M1-USED	5	10	20	30	
Onset	Temp. °C	T_{onset}	222.0	216.8	227.0	257.9	Temp. °C	T_{onset}	220.1	227.1	212.9	278.6
	DTG/%min ⁻¹		-0.40	-0.06	-0.07	-1.01	DTG/%min ⁻¹		-0.33	-0.41	-0.03	-3.30
	TG/%		95.67	98.15	96.59	99.28	TG/%		99.95	99.20	99.43	95.63
	Time/min		39.40	19.18	10.10	7.76	Time/min		39.02	20.21	9.40	8.45
Inflection	Temp. °C	T_{ig}	228.2	244.4	265.2	273.1	Temp. °C	T_{ig}	235.7	248.6	321.8	351.1
	DTG/%min ⁻¹		-1.17	-2.73	-4.59	-5.60	DTG/%min ⁻¹		-1.60	-4.08	-15.45	-26.51
	TG/%		94.87	97.04	95.11	98.98	TG/%		97.35	95.22	79.90	65.86
	Time/min		40.64	21.94	12.01	8.27	Time/min		42.14	22.36	14.84	10.87
Peak	Temp. °C	T_p	288.4	320.0	367.7	390.6	Temp. °C	T_p	303.0	312.6	371.0	395.3
	DTG/%min ⁻¹		-8.62	-15.39	-27.73	-36.48	DTG/%min ⁻¹		-6.16	-15.49	-27.97	-40.32
	TG/%		32.07	30.81	19.48	24.72	TG/%		45.88	34.90	29.20	22.26
	Time/min		52.68	29.50	17.14	12.19	Time/min		55.60	28.76	17.30	12.34
Endset	Temp./°C	T_b	303.4	345.3	388.5	418.7	Temp./°C	T_b	352.5	334.5	395.5	420.9
	DTG/%min ⁻¹		-2.77	-3.04	-4.68	-4.81	DTG/%min ⁻¹		-0.61	-3.99	-4.09	-5.04
	TG/%		15.07	7.02	1.70	4.52	TG/%		10.01	13.57	8.45	2.31
	Time/min		55.68	32.03	18.18	13.12	Time/min		65.50	30.95	18.53	13.20
		M2	5	10	20	30	M2-USED	5	10	20	30	
Onset	Temp. °C	T_{onset}	226.4	241.5	263.1	267.0	Temp. °C	T_{onset}	213.4	232.0	257.0	269.2
	DTG/%min ⁻¹		-0.57	-0.48	-0.24	-1.01	DTG/%min ⁻¹		-0.27	-0.66	-1.27	-1.94
	TG/%		99.16	96.70	98.43	99.48	TG/%		99.57	99.16	98.33	97.89
	Time/min		40.28	21.65	11.91	8.07	Time/min		37.68	20.70	11.60	8.14
Inflection	Temp. °C	T_{ig}	261.8	260.4	322.2	311.5	Temp. °C	T_{ig}	229.2	307.2	309.7	313.5
	DTG/%min ⁻¹		-3.02	-2.59	-10.42	-8.47	DTG/%min ⁻¹		-1.00	-4.83	-9.15	-8.55
	TG/%		88.83	94.20	80.65	94.17	TG/%		98.84	82.10	87.15	90.98
	Time/min		47.36	23.54	14.86	9.55	Time/min		40.84	28.22	14.24	9.62
Peak	Temp. °C	T_p	292.5	368.6	385.1	410.4	Temp. °C	T_p	340.7	368.2	381.1	412.0
	DTG/%min ⁻¹		-4.34	-12.17	-25.14	-32.49	DTG/%min ⁻¹		-4.83	-13.12	-23.60	-35.47
	TG/%		65.71	29.39	33.69	40.91	TG/%		36.99	34.38	35.91	35.40
	Time/min		53.50	34.36	18.01	12.85	Time/min		63.14	34.32	17.81	12.90
Endset	Temp. °C	T_b	349.5	382.4	403.9	433.2	Temp. °C	T_b	361.7	382.6	400.5	435.8
	DTG/%min ⁻¹		-0.60	-2.45	-4.16	-4.66	DTG/%min ⁻¹		-0.68	-1.85	-4.24	-4.48
	TG/%		34.21	18.36	18.83	26.50	TG/%		24.27	22.39	21.30	18.56
	Time/min		64.90	35.74	18.95	13.61	Time/min		67.34	35.76	18.78	13.69

Italics in Table are appropriately applied

TG curves (Fig. 1) showed that zeolite addition into the PP matrix slowed the degradation reaction. However, silver-exchanged zeolite addition into the matrix may accelerate the reaction. Namely, with increasing the silver (Ag) concentration, the onset temperature of degradation shifted to slightly higher values [11]. It was identified that the M2 sample has the T_{onset} values higher than those for M1 sample. For combustion process of M2 type face mask, the following values of T_{onset} degradation temperatures were obtained: 226.4 °C (5 K min⁻¹), 241.5 °C (10 K min⁻¹), 263.1 °C (20 K min⁻¹) and 267.0 °C (30 K min⁻¹). The value of T_{onset} = 226.4 °C at the lowest heating rate used, compared to the literature report corresponds to T_{onset} value for thermal degradation

of PP-zeolite composites (where clinoptilolite as a natural zeolitic tuff, was used as the filler material in the composites) with higher concentration of Ag⁺ ions. In this manner, it can be assumed that in the case of M2 face mask samples, the silver ions are attached to the zeolite. Therefore, surface templated and supported silver nanoparticles form on silver-exchanged mineral upon the thermal reduction. Higher concentrations of silver can represent actually thermo-stable, uniform silver nano-particulates that may have applications as catalysts. However, the identified silver in the M2 type face mask [12] can be highly twinned. The twinned nature of the particles may influence on the increased thermal stability of the M2 sample compared to the M1 sample, during

their degradation under the oxidative conditions. It should be emphasized that PP is much more susceptible to thermal degradation in the presence of silver-exchanged zeolite than in the presence of pure zeolite, which is dictated by the silver concentration level in considered material [13].

The main combustion parameters such as the reactivity (R_M), the ignition index (D_i), the burnout index (D_f), the combustion performance index (S), and the combustion stability index (R_W) for all considered samples are shown in Table 5. For mathematical expressions related to R_M , D_i , D_f , S , and R_W can be referred to ref. [11].

Considering all tested face mask samples, the reactivity (R_M) values are higher for M1/M1-USED samples than R_M values attached to M2/M2-USED samples at all heating rates, which agrees with previous discussion presented above. The reactivity is significantly conditioned by reactions in volatile combustion zones of studied samples, in the temperature range of 250–450 °C (Fig. 1). The higher reactivity values were noticed for M1 and M1-USED samples, where temperature ranges of 250–430 and 440–550 °C can be attributed as devolatilization and char-CO₂ reaction zones, respectively. The reasons behind differences in the reactivity profile of M1/M1-USED and M2/M2-USED face masks are: (1) physical characteristics, (2) elemental and structural components, (3) moisture content, and (4) char combustion rate. Comparing all tested samples, the highest

value of D_i was identified for M1 sample, at all used heating rates. This means that M1 shows such thermal possibility to be combusted (considered M1 as the fuel) in the first stage which was determined by the amount of separated volatile compounds, indicating more efficient and the stable combustion process. On the other hand, the addition of aluminosilicate exchanged metallic ions mineral (i.e., the zeolite—clinoptilolite) into the face mask (such as M2 type of face mask), decreased the “stability” of the degradation process (for example, at $\beta=20 \text{ K min}^{-1}$ for M1, $D_i=1.35 \times 10^{-1}$, and for M2, $D_i=9.40 \times 10^{-2}$ (Table 5)). The burnout index (D_f) was dependent on the burnout temperature. The lower the D_f value was, the more time and the higher treatment temperature were needed to complete the burnout at the same heating rate. The combustion processes of zeolite-rich face masks (M2 and M2-USED) are characterized by the lower D_f values (Table 5). The combustion performance index (S) had the same trend as D_i , which corresponded to higher combustion activity with the rise of the value of the S index (Table 5). The S increased with the rise of maximum mass loss (DTG_{max}) (Fig. 1). The addition of zeolite (adsorptive and exchangeable material) to face mask caused a decrease of S , which corresponded to the decreased combustion activity (Table 5). Comparing all tested samples, lower values of R_W were observed at lower heating rates ($\leq 10 \text{ K min}^{-1}$), while combustion stability index almost triples achieving

Table 5 Main combustion parameters for M1, M1-USED, M2, and M2-USED samples

Sample/Heating rate	Reactivity R_M	Ignition index D_i	Burnout index D_f	Combustion performance index S	Combustion stability index R_W
	% °C ⁻¹ min ⁻¹	% min ⁻³	% min ⁻⁴	% ² °C ⁻³ min ⁻²	–
M1					
5 K min ⁻¹	1.535	4.03×10^{-3}	8.68×10^{-5}	9.67×10^{-6}	4.603
10 K min ⁻¹	2.595	2.38×10^{-2}	8.91×10^{-4}	2.55×10^{-5}	6.334
20 K min ⁻¹	4.328	1.35×10^{-1}	8.90×10^{-3}	7.22×10^{-5}	9.542
30 K min ⁻¹	5.497	3.62×10^{-1}	3.31×10^{-2}	1.16×10^{-4}	11.855
M1-USED					
5 K min ⁻¹	1.069	2.63×10^{-3}	4.82×10^{-5}	4.21×10^{-6}	3.893
10 K min ⁻¹	2.645	2.41×10^{-2}	9.34×10^{-4}	2.93×10^{-5}	6.366
20 K min ⁻¹	4.343	1.09×10^{-1}	7.06×10^{-3}	8.36×10^{-5}	9.503
30 K min ⁻¹	6.033	3.01×10^{-1}	2.73×10^{-2}	1.75×10^{-4}	12.756
M2					
5 K min ⁻¹	0.767	1.71×10^{-3}	3.17×10^{-5}	2.78×10^{-6}	3.368
10 K min ⁻¹	1.897	1.50×10^{-2}	5.05×10^{-4}	1.54×10^{-5}	5.349
20 K min ⁻¹	3.820	9.40×10^{-2}	5.95×10^{-3}	6.23×10^{-5}	8.716
30 K min ⁻¹	4.754	2.65×10^{-1}	2.34×10^{-2}	9.18×10^{-5}	10.682
M2-USED					
5 K min ⁻¹	0.787	1.87×10^{-3}	3.34×10^{-5}	2.57×10^{-6}	3.478
10 K min ⁻¹	2.046	1.35×10^{-2}	4.55×10^{-4}	1.76×10^{-5}	5.521
20 K min ⁻¹	3.608	9.31×10^{-2}	5.95×10^{-3}	5.75×10^{-5}	8.327
30 K min ⁻¹	5.178	2.86×10^{-1}	2.51×10^{-2}	1.08×10^{-4}	11.481

the highest heating rate (30 K min^{-1}). Therefore, based on these results, it could be recommended the implementation of combustion process of these materials at the lower heating rates (at or below 10 K min^{-1}). Finally, the trend of D_i and D_f indices was in accordance with the S index, presenting higher values for M1/M1-USED samples, thus confirming their better combustion properties. Additionally, as shown in Tables 3 and 5, for the high ash fuel (M2 and M2-USED face masks), the combustion properties get worse. So, obviously, the M1 and M1-USED samples show much better ignition performances than M2/M2-USED samples.

Evolved gas analysis (EGA) using mass spectrometry (MS) measurements during face masks combustion process

Figures 2 and 3a–d show simultaneous DTG-MS profiles of M1 and M2 face masks during combustion process at $\beta = 10 \text{ K min}^{-1}$ including: (a) water (H_2O) MS signals, (b) carbon dioxide (CO_2) MS signals, (c) the light hydrocarbons

MS signals, and (d) hydrogen cyanide (HCN) MS signals. The corresponded DTG-MS profiles for other face mask samples (“USED”) are not shown, because their profiles/signals are very similar to the previous samples mentioned above.

Considering both samples, the water vapor starts to release at about $220 \text{ }^\circ\text{C}$ with further, the rapid increasing of the ion current signals in MS spectrum, reaching a maximum at around 325 and $380 \text{ }^\circ\text{C}$ (Figs. 2 and 3a), respectively. The water vapor starts to release at temperatures slightly higher than those at which polypropylene (PP) exhibits fall in properties such as strength and viscosity (in a melt) ($\sim 160/165 \text{ }^\circ\text{C}$). As the temperature of the melted PP increases, the endothermic thermal degradation starts by random scission process, which is essentially the break-up of weakest carbon–carbon links in the carbon backbone, thus resulting in a progressive reduction in the molecular weight (MW). This process is called “thermal pyrolysis”. Further reduction in MW eventually leads to molecules that are small enough to volatilize. In the above-indicated

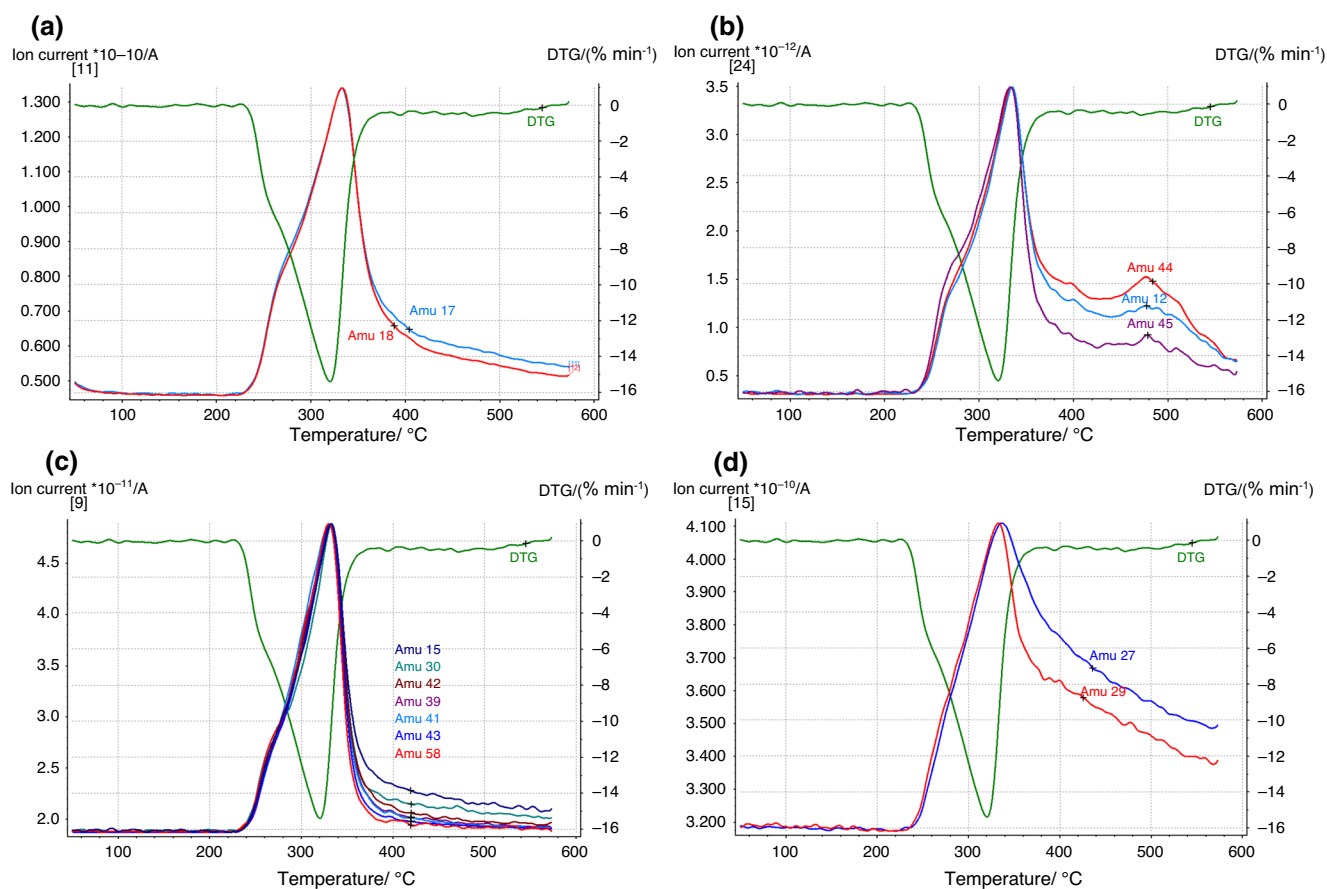


Fig. 2 DTG-MS profiles of M1 face mask thermo-oxidative degradation in an air atmosphere at 10 K min^{-1} : **a** amu 17, amu 18—fragment and main MS signals for water vapor: H_2O , **b** amu 12, amu 45 and amu 44—fragments and main MS signals for carbon dioxide:

CO_2 , **c** amu 15, amu 30, amu 42, amu 39, amu 41, amu 43 and amu 58—fragments and main MS signals for light hydrocarbons ($\text{C}_1\text{--C}_4$), and **d** amu 29, amu 27—fragment and main MS signals for hydrogen cyanide: HCN

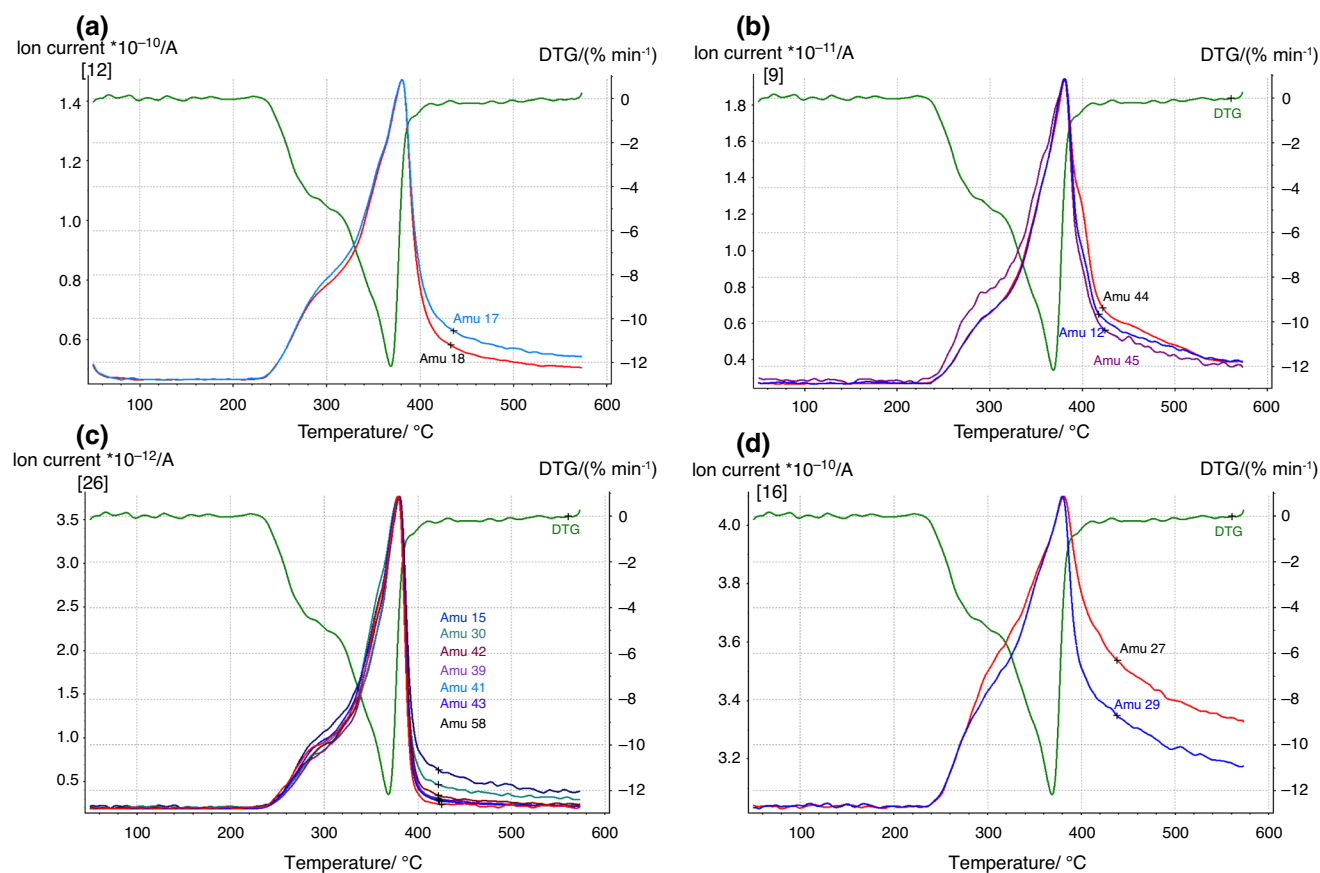


Fig. 3 DTG-MS profiles of M2 face mask thermo-oxidative degradation in an air atmosphere at 10 K min^{-1} : **a** amu 17, amu 18—fragment and main MS signals for water vapor: H_2O , **b** amu 12, amu 45 and amu 44—fragments and main MS signals for carbon dioxide:

CO_2 , **c** amu 15, amu 30, amu 42, amu 39, amu 41, amu 43 and amu 58—fragments and main MS signals for light hydrocarbons ($\text{C}_1\text{--C}_4$), and **d** amu 29, amu 27—fragment and main MS signals for hydrogen cyanide: HCN

temperatures where MS signals reach maximum ion current values (Figs. 2 and 3a), the energetic volatile species are produced together with releasing of water vapor as additional product as a consequence of PP degradation [14]. Moving MS signal for H_2O liberation to higher temperature for M2 sample, it is in accordance with its enhanced thermal stability under oxidative conditions.

Positioned at the same maximum temperatures where H_2O MS-signals occur, many successfully aligned/overlapping MS signals similar to H_2O MS-signals take place, and they can be attributed to product distributions in non-condensable permanent gases produced from investigated face masks (Figs. 2 and 3c). The gases were methane (CH_4 , amu 15 fragments), ethane (C_2H_6 , amu 30), propane (C_3H_8 , 42 amu), propylene (C_3H_6 , amu's 39 and 41 fragments), and butane (C_4H_{10} , amu's 58 and 43). The propylene (C_3H_6) represents most produced non-condensable gas for thermal degradation of face masks, which obviously resulted from depolymerization of PP that comprises mask filter layers. It should be noted that $\text{C}_1\text{--C}_4$ hydrocarbons are rapidly accumulated, i.e., the volatile fraction appeared

to increase with an increase of temperature from 275/280 to 310 °C, where these temperatures correspond to locations of “shoulders” appearing, which was attributed to the thermal degradation of fibrous (cellulose) components of masks (Figs. 2 and 3c). Namely, as the temperature increased, detangled element between the milled particles was removed and friction-mechanical bonds between fabrics were dismantled and converted into individual microparticles (about $T \sim 280$ °C) in the form of debris and damaged microparticles. Further, the penetration of the produced heat flux inside damaged particles can be followed by breaking of β -1,4-glycosidic bonds of cellulose/hemicellulose molecules forming small molecules and some amorphous regions at elevated temperature (approximately 420 °C) [15]. Emphasized transformations may characterize DTG curves behavior up to previously indicated temperature, but these changes probably take place in a concurrent manner with PP thermal conversion. As a consequence of this, the current forms of DTG curves are generated (and thus MS-signals) which correspond to the presence of overlapping reactions. Additionally, CH_4

and the CO₂ (Figs. 2 and 3c and Figs. 2 and 3b) could be produced via thermal cracking of pyrolytic vapor. Furthermore, releases of carbon dioxide (CO₂) occurs at 'two maximum temperatures' related to MS-signals for M1 sample, and at 'one maximum temperature' related to MS-signals for M2 sample, with a stronger ion current (Figs. 2 and 3b).

For M1 sample, the occurrence of MS signals related to CO₂ evolution (Fig. 2b) can be explained by major constituents of M1 face mask (i.e., the polypropylene (PP) in a larger amount and nylon 6 in a smaller amount, considering the mask rope) that have limited quantity of the oxygen (Table 3), and the high quantity of carbon monoxide (CO) cannot be expected without presence of CO₂ as an oxygen source. TG results (Fig. 1a) confirms that no additional heterogeneous reactions between CO₂ and solid face mask were occurred. The explanation for appearance of MS signals with amu's 44, 45, and 12 at about 490 °C (Fig. 2b) can be attributed to gas-phase homogeneous reactions (GPRs) between CO₂ and gaseous hydrocarbons evolved from devolatilization (pyrolysis) through second heating zone (Fig. 2c) of combustion process at about 500 °C. Since that ion current of gaseous effluents is not negligible for the region which begins at $T=420$ °C and beyond, therefore, it can be inferred that CO formation was not entirely ascribed to reverse water–gas shift reaction and CO₂ dry reforming, thereby suggesting an additional GPRs between CO₂ and gaseous hydrocarbons evolved from M1 face mask pyrolysis. Consequently, CO₂ may acts as soft oxidant for catalytic behavior [16] of studied process. Therefore, the MS signal with amu 12 can be attributed to MS-fragment of CO molecule at $T\sim 490$ °C (Fig. 2b)). MS spectrum for M2 sample does not show additional MS signals at temperatures above 420 °C (Fig. 3b) eliminating events described-above, since that M2 face mask is not limited to oxygen quantity (Table 3) and with the presence of a larger amount of the ash offered the solid carbon residue. However, above-described mechanism is probably hindered by morphology properties of the produced solid carbon [17].

Considering both samples (M1 and M2), MS signals with amu's 29 and 27 situated at the maximum temperature values around 350 and 390 °C (Figs. 2 and 3d) can be attributed to devolatilized product, hydrogen cyanide (HCN) (inorganic substance), arising from thermal degradation of nylon 6 compound as the major component for the mask rope within an ear strap's [18, 19]. It should be emphasized that in the devolatilization stage, the disproportionation reaction of propylene can result in the formation of ethylene (C₂H₄) [20]. The disproportionation reaction can thermally eventuate producing the lower selectivity than catalytic reaction which can also take place. Figure 4 shows DTG-MS profiles of the M1 face

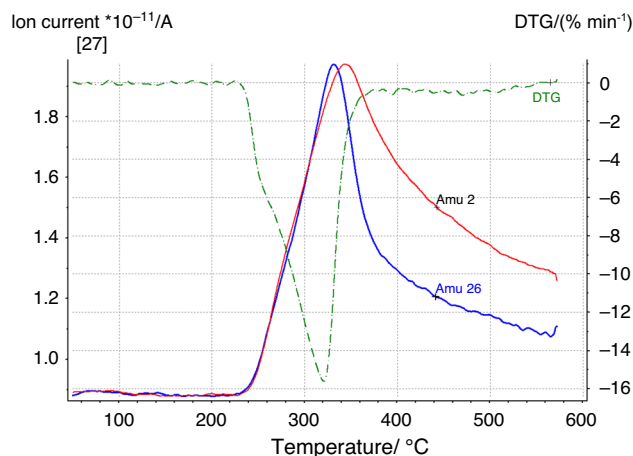


Fig. 4 DTG-MS profiles of M1 face mask at 10 K min^{-1} with amu 26 (ethylene fragment) and amu 2 (hydrogen)

mask at $\beta=10\text{ K min}^{-1}$, where amu's 26 and 2 were identified for ethylene fragment and the evolved hydrogen gas (H₂).

It can be observed from Fig. 4 that both MS profiles, with amu's 26 and 2, are almost matching up to approximately 350 °C, where after this temperature there is a significant divergence in MS-signals for identified chemical species. Thus, above the mentioned temperature, the presence of both species cannot be claimed with great certainty.

Obviously, the generation of H₂ follows the creation of ethylene where the disproportionation reaction [20, 21] is thermally triggered with probably an absence of active catalyst, and where hydrogen generation occurs through dehydrogenation reactions within pyrolysis stage. Therefore, it can be expected that hydrogenation of ethylene with the hydrogen generated during the pyrolysis stage can produce the lower hydrocarbons such as ethane and propane which were formerly identified (Fig. 2). Since the M2 and M2-USED face masks yield a much more nonvolatile solid residue (i.e., the char) compared to M1 and M1-USED face masks (Fig. 1a–d), it can be assumed that this product is formed in pyrolytic stage, where volatiles can evolve via parallel and serial reactions occurring homogeneously or heterogeneously, which may result in the formation of complex mixture of products. Consequently, based on the established results, the thermochemical conversion processes of protective face masks can convert these waste polymer-based materials into useful energy-yielding products. So, the designing of operative gasification can lead to production of syngas and hydrogen fuel production. In that context, these energy-yield products may help to compensate for fossil fuels depletion in a near future.

Conclusions

The sudden increase in coronavirus face masks during COVID-19 pandemic underlines the crucial need for a proper disposal method, so they do not end up in landfills, posing a hazard. In this work, waste-to-energy (WTE) route was examined in order to assess valorization of coronavirus protective face masks (consider rather as domestic waste nor medical waste) for production of gaseous fuels via thermochemical process such as combustion, using simultaneous TG-DTG-MS techniques. The two types of protective face masks are used in this study: surgical (disposable) coronavirus face masks (M1/M1-USED), and coronavirus protective commercial face masks (M2 and M2-USED), riches with natural zeolite–clinoptilolite: silver-ion-exchanged zeolite.

Thermogravimetric analysis showed a thermo-oxidative degradation stages and temperatures for all face masks. Thermogravimetry (TG)-derivative thermogravimetry (DTG) analyses have shown apparently that the combustion process proceed through the single-stage mechanism related to the thermo-oxidative degradation of polypropylene (PP) as the major constituent of tested masks. However, based on the closer inspection of obtained TG-DTG features, it was founded that additional “shoulder peaks” occur at different heating rates, for all tested samples. This behavior can be attributed to overlapping reactions which take place during thermal degradation of fibrous material (predominantly cellulosic–cotton-like nanofibers) which is in composition of the inner layer of face masks. The DTG curves for M2/M2-USED samples are smaller compared to DTG curves related to M1/M1-USED samples that was a consequence of the devolatilization, and which progressed more slowly. Considering the established T_p (maximum peak temperature) and T_b (burnout temperature) values which were higher for unused and used M2 type of face mask than T_p and T_b values for M1 and M1-USED samples, it was concluded that both M2 face masks exhibit the lower reactivity compared to M1 face masks. This may have been caused by a higher content of inorganic matter presented in the M2 type of face mask, which possibly had an influence on the heat transfer in the testing thermobalance chamber ambience. The higher values of burnout temperatures for M2/M2-USED samples resulted from the difficulty of burning of these samples, which caused a longer combustion time and a higher burnout temperature to complete the conversion process. The trend of D_i and D_f indices was in accordance with the S index, presenting higher values for M1/M1-USED, thus confirming their better combustion properties. Additionally, for silver-ion-exchanged zeolite contained face masks which have more ash content, the combustion properties were worsened.

For observed samples, it was established that TG results show that the most heat is generated above 325 °C favoring lower heating rates. Therefore, to ensure that thermal utilization of face masks waste is effective while maintaining proper energy management, it should be carried out in the temperature range from 325 °C to approximately 550 °C. Additionally, it was revealed that for the M1 face mask sample, the exposed carbon dioxide (CO₂) acts as a soft oxidant for catalytic combustion process at about 490 °C in the presence of CO, suggesting gas phase homogeneous reactions (GPRs) between CO₂ and gaseous hydrocarbons evolved from devolatilization stage. This work provides future guides for energy valorization of protective coronavirus face masks with and without silver nanoparticles (classified also as antimicrobial face mask) by thermochemical processing such as combustion, including thermal analysis testing methods. Conclusions drawn from this research can help in design and development of combustion reactors for this type of waste materials.

Authors' contributions NM contributed to investigation, data curation, methodology, writing—original draft, writing—review and editing, and supervision. BJ contributed to conceptualization, formal analysis, writing—original draft, writing—review and editing, visualization, and supervision. DS contributed to investigation, validation, data curation, and supervision. PA contributed to investigation, validation, visualization, and supervision. MR contributed to investigation, data curation, and supervision. All authors contributed to the study conception and design.

Funding The research was funded by the Ministry of Education, Science and Technological Development of the Republic of Serbia contracts no. 451–03–68/2022–14/200105 (N. Manić) and no. 451–03–68/2022–14/200017 (B. Janković).

Availability of data and materials The datasets generated during and/or analyzed during the current study are available from the corresponding author on reasonable request.

Code availability Not applicable.

Declarations

Conflict of interest The authors declare that they have no known competing financial interests or personal relationships that could have appeared to influence the work reported in this paper.

References

- Jain S, Lamba BY, Kumar S, Singh D. Strategy for repurposing of disposed PPE kits by production of biofuel: Pressing priority amidst COVID-19 pandemic. *Biofuels* August 2020, <https://doi.org/10.1080/17597269.2020.1797350>.
- Ciuffreda S, Picotti C, Pescio P. Medical face masks on the market: Review of materials, characteristics and performed tests,

- Eurofins Biolab Srl – via B.Boozzi 2, Vimodrone (Milano), Italy, Eurofins Medical Device Testing, 2020.
- Jung S, Lee S, Dou X, Kwon EE. Valorization of disposable COVID-19 mask through the thermo-chemical process. *Chem Eng J.* 2021;405: 126658. <https://doi.org/10.1016/j.cej.2020.126658>.
 - Varghese PJG, Anna David D, Karuth, A, Fatima Manamkeri Jafferli, J, Begum P M S, Jacob George J, Rasulev B, Raghavan, P. Experimental and Simulation Studies on Nonwoven Polypropylene-Nitrile Rubber Blend: Recycling of Medical Face Masks to an Engineering Product, *ACS Omega.* 2022;7:4791–803.
 - Giakoumakis G, Politi D, Sidiras D. Medical waste treatment technologies for energy, fuels, and materials production: A review. *Energies.* 2021;14(23):8065. <https://doi.org/10.3390/en14238065>.
 - ISO 21640:2021, Solid recovered fuels—specifications and classes, International Organization for Standardization, 2021, Geneva, Switzerland.
 - Radojević M, Janković B, Stojiljković D, Jovanović V, Čeković I, Manić N. Improved TGA-MS measurements for evolved gas analysis (EGA) during pyrolysis process of various biomass feedstocks. Syngas energy balance determination. *Thermochim Acta.* 2021;699: 178912. <https://doi.org/10.1016/j.tca.2021.178912>.
 - Aich S, Behera D, Nandi BK, Bhattacharya S. Relationship between proximate analysis parameters and combustion behaviour of high ash Indian coal. *Int J Coal Sci Technol.* 2020;7:766–77. <https://doi.org/10.1007/s40789-020-00312-5>.
 - Calorific value of waste. Calorific value (CV) of waste, Available at: <http://www.igniss.com/calorific-value-waste>.
 - Majewsky M, Bitter H, Eiche E, Horn H. Determination of microplastic polyethylene (PE) and polypropylene (PP) in environmental samples using thermal analysis (TGA-DSC). *Sci Total Environ.* 2016;568:507–11. <https://doi.org/10.1016/j.scitotenv.2016.06.017>.
 - Samper MD, Bertomeu D, Arrieta MP, Ferri JM, López-Martínez J. Interference of biodegradable plastics in the polypropylene recycling process. *Materials.* 2018;11:1886. <https://doi.org/10.3390/ma11101886>.
 - Blevens MS, Pastrana HF, Mazzotta HC, Tsai CS-J. Cloth face masks containing silver: Evaluating the status. *ACS Chem Health Saf.* 2021;28(3):171–182. <https://doi.org/10.1021/acs.chas.1c00005>
 - Pehlivan H, Balköse D, Ülkü S, Tihminhoğlu F. Effect of zeolite filler on the thermal degradation kinetics of polypropylene. *J Appl Polym Sci.* 2006;101(1):143–8. <https://doi.org/10.1002/app.23105>.
 - Khoury GA, Willoughby B. Polypropylene fibres in heated concrete. Part 1: Molecular structure and materials behavior. *Magaz Concr Res.* 2008;60(2):125–36. ISSN 0024–9831; <https://doi.org/10.1680/macr.2008.60.2.125>
 - Gupta A, Thengane SK, Mahajani S. Kinetics of pyrolysis and gasification of cotton stalk in the central parts of India. *Fuel.* 2020;263: 116752. <https://doi.org/10.1016/j.fuel.2019.116752>.
 - Rahman ST, Choi J-R, Lee J-H, Park S-J. The role of CO₂ as a mild oxidant in oxidation and dehydrogenation over catalysts: A review. *Catalysts.* 2020;10(9):1075. <https://doi.org/10.3390/catal10091075>.
 - Chen R, Zhang D, Xu X, Yuan Y. Pyrolysis characteristics, kinetics, thermodynamics and volatile products of waste medical surgical mask rope by thermogravimetry and online thermogravimetry-Fourier transform infrared-mass spectrometry analysis. *Fuel.* 2021;295: 120632. <https://doi.org/10.1016/j.fuel.2021.120632>.
 - Brillard A, Kehrli D, Douguet O, Gautier K, Tschamber V, Bueno M-A, Brillhac J-F. Pyrolysis and combustion of community masks: Thermogravimetric analyses, characterizations, gaseous emissions, and kinetic modeling. *Fuel.* 2021;306: 121644. <https://doi.org/10.1016/j.fuel.2021.121644>.
 - Dixon RE, United States patent 3485890A, 1969.
 - Fogler HS. *Elements of Chemical Reaction Engineering*, 4th Ed., Chaps. 2–4, Prentice-Hall, Upper Saddle River, NJ, 2006.
 - Hill CG Jr, Root TW. *Introduction to chemical engineering kinetics and reactor design*, 2nd Ed., Ch. 8. Wiley, New York, 2014.

Publisher's Note Springer Nature remains neutral with regard to jurisdictional claims in published maps and institutional affiliations.